Novel model for propagation loss prediction in tunnels

Zhang, Yue Ping

2003

Zhang, Y. P. (2003). Novel model for propagation loss prediction in tunnels. IEEE Transactions on Vehicular Technology. 52(5), 1308-1314.

https://hdl.handle.net/10356/91426

https://doi.org/10.1109/TVT.2003.816647

Novel Model for Propagation Loss Prediction in Tunnels

Y. P. Zhang

***Abstract*—Radio signal propagation in a tunnel exhibits distinct near and far regions with quite different propagation characteristics. This paper proposes a model that can distinguish these propagation regions and predict their respective propagation losses in the tunnel. The model relies on a break point to separate the propagation regions and a hybrid technique to calculate the propagation losses. The location of the break point is determined with the solution of a novel tunnel-propagation equation for the first time. The solution shows that the location of the break point depends strongly upon frequency, antenna position, and tunnel transversal dimensions. The model is compared with data measured in various tunnels at different frequencies (900 MHz, 1.8 GHz, and 2.448 GHz). The results show reasonable agreement between predictions and measurements.**

***Index Terms*—Mobile communications, radio propagation.**

I. Introduction

THERE EXIST two regions separated by a break point for radio signal propagation along a line-of-sight (LOS) path in rural, suburban, or urban environments. Propagation in these two regions has quite different characteristics. Before the break point is the near region where the propagation loss is smaller. After the break point is the far region where the propagation loss is larger. A formula to calculate the location of the break point is available and expressed as a simple function of wavelength and antennas' heights [1], [2]. The formula is useful to define the size of a microcell and to design for fast handover. Similarly, two propagation regions separated by a break point are also observed along a LOS path in a tunnel. On the contrary, the propagation loss is larger in the near region and smaller in the far region of the tunnel. This implies that the available formula to locate the break point is inapplicable in tunnel environments. Therefore, how to distinguish these two regions and how to predict their respective propagation losses in the tunnel are worth investigation. A detailed study of the technical literature reveals that some work relevant to the problems has been published, but that the available limited information is still generally inconsistent and ambiguous [3]–[6]. Of the references cited here, [3] and [4] are related to calculating the propagation losses, whereas [5] and [6] to identifying the propagation regions. Deryck reports that the propagation losses in the near and far regions agreed with the specific attenuation rates of the transverse electric $(\mathrm{TE})_{11}$ and TE_{10} modes, respectively [3]. Delogne describes that the $E_{0\mathrm{n}}^{(v)}$ modes were dominant in the near region and the $E_{\mathrm{mn}}^{(h)}$ mode were dominant in the far region for a radio link with both vertically polarized transmitting and receiving antennas. The propagation losses fit with the specific attenuation rate of the $E_{01}^{(v)}$ modes in the near region and with that of $E_{00}^{(h)}$ mode in the far region [4]. Klemenschits and Bonek use a critical distance parameter to distinguish the regions to establish their measurement-based tunnel-propagation model. They found that the critical distance was directly proportional to the square of the largest cross dimension of a tunnel and inversely proportional to wavelength [5]. Lienard and Degauque introduce a distance parameter to distinguish the regions to study the statistical propagation characteristics. They mention that the distance parameter might vary from 50 to 100 m. In the case of a dipole antenna placed in a tunnel, the distance parameter was close to 50 m [6].

In this paper, the usual term of the break point to distinguish two propagation regions in a tunnel is adopted. In Section II, a simple tunnel-propagation model is proposed, the break point is defined, and a novel approach to locate it is described. In Section III, the comparison of the model predictions with the measurements is presented. Agreement is achieved in various tunnels at 900 MHz, 1.8 GHz, and 2.448 GHz. In addition, the location of the break point affected by changes in frequency, antenna parameters, and tunnel measures are analyzed and discussed. Finally, Section IV gives conclusions.

II. Tunnel-Propagation Model

A tunnel of width w meters and height h meters is surrounded by a lossy nonmagnetic homogeneous medium with relative permittivity ε_r and conductivity σ. Inside the tunnel an antenna $\mathrm{T_x}$ is located at point (x_t, y_t, z_o) to excite a radio signal and another antenna $\mathrm{R_x}$ is placed at point (x_r, y_r, z) to receive the radio signal. The origin of the tunnel-coordinate system is arranged at the middle of the tunnel cross section. For the tunnel whose cross-sectional dimensions are sufficiently greater than a free-space wavelength λ, the ray optical models have been developed to predict the propagation loss. The fundamental ray optical model is expressed as

$$\begin{aligned}\mathrm{PL\ (dB)} &= 10\log_{10}\left(\frac{P_t}{P_r}\right)\\ &= 10\log_{10}\left(\left(\frac{\lambda}{4\pi}\right)^2\left|\frac{G_d}{r}\right.\right.\\ &\qquad\left.\left.+\sum_{i=1}^{\infty}\frac{G_iR_i\exp\left(j\frac{2\pi}{\lambda}(r_i-r)\right)}{r_i}\right|^2\right)\end{aligned}\tag{1}$$

Manuscript received June 22, 2001; revised May 7, 2003.

The author is with the Integrated Systems Research Laboratory, School of Electrical and Electronic Engineering, Nanyang Technological University, Singapore, Singapore (e-mail: eypzhang@ntu.edu.sg).

Digital Object Identifier 10.1109/TVT.2003.816647

where G_d and G_i are the products of the transmitting and receiving antenna field amplitude radiation patterns corresponding to the paths of the direct and the ith reflected ray, respectively; R_i is the product of the reflection coefficients of all the walls where the ith ray suffers reflection; and r and r_i are the path lengths of the direct and the ith reflected ray. This model can calculate the variation of the propagation loss on a wavelength scale. The propagation losses in both the near and far regions of the tunnel can be accurately predicted; however, the implementation of the model requires heavy computation [7]–[10]. The analytical ray optical (waveguide) model is given by

$$\begin{aligned}\mathrm{PL}_f\ (\mathrm{dB}) &= 10\log_{10}\left(\frac{P_t}{P_r}\right)\\ &= 5\lambda r\left(\frac{1}{w^2}\log_{10}\frac{1}{|R_1|^2}+\frac{1}{h^2}\log_{10}\frac{1}{|R_2|^2}\right)\\ &\quad+\mathrm{CL}_t+\mathrm{CL}_r\end{aligned}\tag{2}$$

where R_1 and R_2 are the reflection coefficients of the tunnel vertical and horizontal walls at the grazing angles $\phi_1=\lambda/2w$ and $\phi_2=\lambda/2h$, respectively, and CL_t and CL_r are the coupling losses of the transmitting and receiving antennas, respectively. The coupling loss for an antenna located at point (x, y) in the tunnel cross section is derived in the Appendix as

$$\mathrm{CL}\ (\mathrm{dB})=10\log\left(\frac{2\pi wh}{\lambda^2 G}\cos^{-2}\left(\frac{\pi x}{w}\right)\cos^{-2}\left(\frac{\pi y}{h}\right)\right)\tag{3}$$

where G is the gain of the antenna. This model is simple to use, but only yields the acceptable prediction for the propagation loss in the far region of the tunnel. Furthermore, where the far region starts in the tunnel is not considered in the model [11], [12]. Therefore, a propagation model that can keep the advantages and discard the disadvantages of the above models is desired. In the following, we will propose such a novel propagation model. For this purpose, we write the single ray optical (free space) model as

$$\mathrm{PL}_n\ (\mathrm{dB})=10\log_{10}\left(\frac{P_t}{P_r}\right)=10\log_{10}\left[\frac{\lambda^2}{(4\pi)^2}\left|\frac{G_d}{r}\right|^2\right].\tag{4}$$

It is known that this model can predict the propagation loss not only for free space, but also for various spaces with the first Fresnel zone clearance.

The ray optical models have been used to calculate the propagation loss for a hypothetical radio link at 2 GHz between two horizontally polarized isotropic antennas in a tunnel with the following parameter values: $w=8$ m; $h=5$ m; $\varepsilon_r=10$; and $\sigma=0.01$ S/m. Fig. 1 shows the results for the transmitting antenna at $(0,0,z_o)$ and the receiving antenna at $(0,0,z)$. The irregular curve represents the simulation of the fundamental ray optical model, while the regular curve represents the single ray optical model and the straight line represents the analytical ray optical model. It is seen from the irregular curve that two propagation regions exist. In the region near the transmitting antenna, the propagation fluctuates rapidly and the propagation loss is larger, while in the region far away from the transmitting antenna, the propagation fluctuates slowly and the propagation loss is smaller. It is also seen that the regular curve generally follows the trend of the irregular curve well in the near region but does so poorly in the far region, while the straight line generally follows the trend of the irregular curve poorly in the near region but well in the far region. The intersection of the regular curve with the straight line can be used to distinguish the two propagation regions. This suggests to us that we propose a tunnel-propagation model as follows. We define the intersection as the break point to distinguish the propagation regions. Before the break point is the near propagation region, which has the first Fresnel zone clearance. The propagation takes place in this region of the tunnel as if it were in free space; the propagation loss is, therefore, calculated by the single ray optical (free space) model. After the break point is the far propagation region, where the constructive interference dominates; the propagation takes place in this region of the tunnel as if it were in a waveguide. The propagation loss is, therefore, calculated by the analytical ray optical (waveguide) model. As for the break point, it is located in the propagation path where the propagation losses from the two models are equal; that is, the first solution of the equation

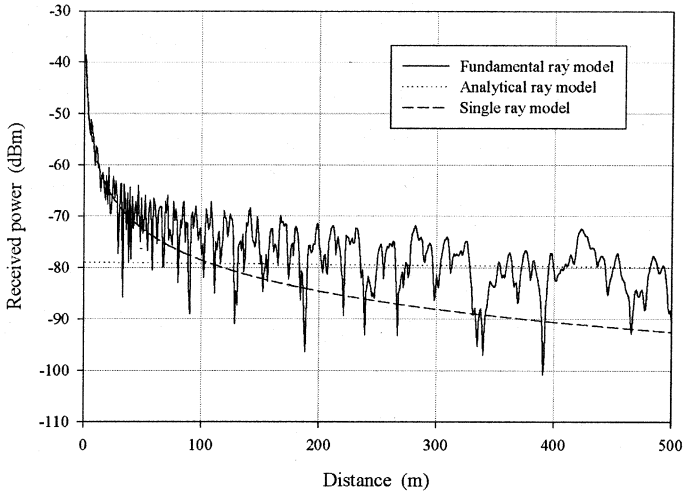

Fig. 1. Simulations of the ray optical models.

$$\mathrm{PL}_n\ (\mathrm{dB})=\mathrm{PL}_f\ (\mathrm{dB})\tag{5}$$

yields the break point.

The model developed so far is for a rectangular tunnel. The model, in fact, can also be used for an other-shaped tunnel. When used for the other-shaped tunnel, the model requires properly determining the equivalent rectangular tunnel. This can be easily done as follows: Let the cross-sectional area of the equivalent rectangular tunnel be the cross-sectional area of the other-shaped tunnel and the width of the equivalent rectangular tunnel be the floor width of the other-shaped tunnel [13].

III. Results and Discussion

For validation purposes, measurements have been made and published experimental data have been collected for various tunnels at different frequencies. In what follows, the measurements

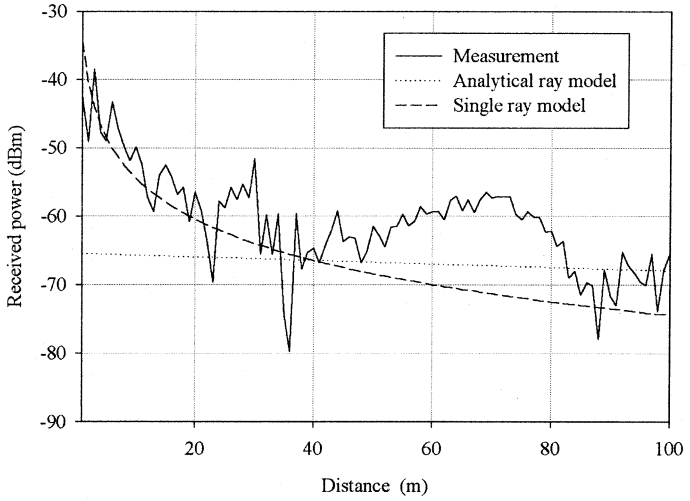

Fig. 2. Measured and predicted received power at 900 MHz in a coal mine tunnel.

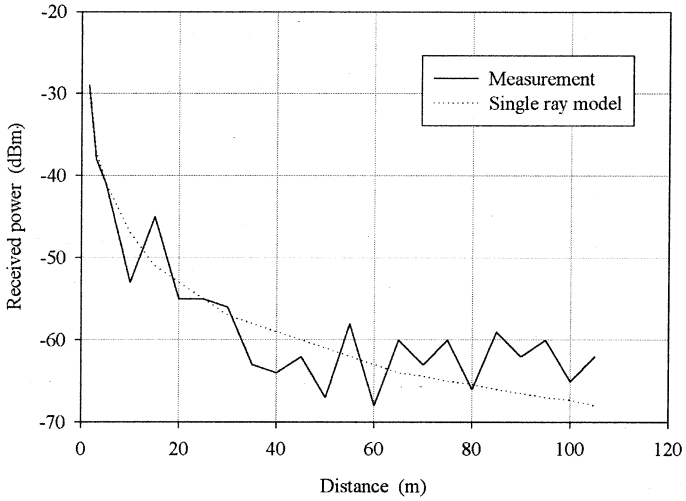

Fig. 3. Measured and predicted received power at 900 MHz in a road tunnel.

are first described and then the comparisons of the predictions with the measurements are presented.

The measurement setup consists of three modules: 1) an HP 44233B signal source used as the transmitter; 2) an R/S ESV signal strength meter used as the receiver; and 3) a pen-written plotter used as the data collector. Both transmitting and receiving antennas were standard dipoles. The measurement setup was calibrated with 120-dB dynamic range. During the measurement campaign, the transmitter was fixed in a selected position of a tunnel. The receiver was being moved at a constant speed along a selected route in the tunnel. The output of the receiver was continuously recorded by the pen-written plotter. In this manner, the variation of received signal power along the route in the tunnel could be visualized immediately to locate the break point. The process was repeated three times for horizontal polarization and three times for vertical polarization. The recorded data were manually digitized and a two-slope regression method was employed to analyze them.

A measurement at 900 MHz in a coal mine tunnel of $w = 4$ m and $h = 3.5$ m is shown in Fig. 2 with the prediction. For this measurement, the transmitting and receiving antennas were horizontally polarized and located at $(-0.35\ w, -0.057h, z_o)$ and $(-0.35\ w, -0.057\ h, z)$, respectively. The two different propagation regions separated at the distance point of approximate 40 m are clearly observed from the measurement. This distance point of 40 m is referred as the measured break point. The received signal power drops quickly before the measured break point and slowly afterward. The general behavior of the received signal power is predicted by the model. In the prediction, the material parameters for the coal mine tunnel were chosen to be $\varepsilon_r = 10$ and $\sigma = 0.01$ S/m [12]. The calculated break point is also at the distance of 40 m. Another measurement at 900 MHz in a road tunnel of $w = 7.5$ m and $h = 4$ m is plotted with the prediction in Fig. 3. For this measurement, the transmitting and receiving antennas were vertically polarized and located at $(0, -0.2\ h, z_o)$ and $(-0.3\ w, -0.2\ h, z)$, respectively. The calculated break point is found at the distance of 150 m. The measurement was thus made all in the near region and only the single ray optical model of our tunnel-propagation model is adequate

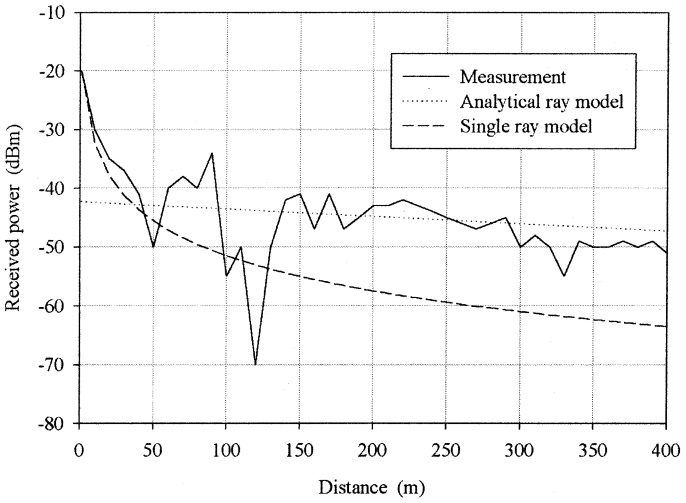

Fig. 4. Measured and predicted received power at 915 MHz in a potash mine tunnel.

for the prediction in this case. The prediction lies within 5 dB of the measurement. Measurements at 915 MHz in a potash mine tunnel are reported in [14]. The tunnel has $w = 8.6$ m, $h = 2.7$ m, $\varepsilon_r = 6$, and $\sigma = 0.0001$ S/m. The transmitting and receiving antennas were located at $(0, 0, z_o)$ and $(0, 0, z)$, respectively. Fig. 4 shows the prediction and measurement for the horizontally polarized radio signal. The calculated break point is at the distance of 40 m and the measured break point is in the vicinity of this distance. The prediction agrees reasonably with the measurement in the regions before and after the calculated break point.

Measurements at two frequencies (945 MHz and 1.853 GHz) in two subway tunnels are reported in [15]. Fig. 5 illustrates, respectively, the predictions and the measurements for the propagation at 945 MHz and 1.853 GHz in the arched subway tunnel. The arched tunnel constituted by a circular shape of radius 2.9 m with an elevated floor 1.2 m above the lowest point of the circle is approximated by a rectangular tunnel with $w = 4.7$ m and $h = 4.7$ m. Note that the measured break points are in the vicinities of 68 m for 945 MHz and 120 m for 1.853 GHz, while the

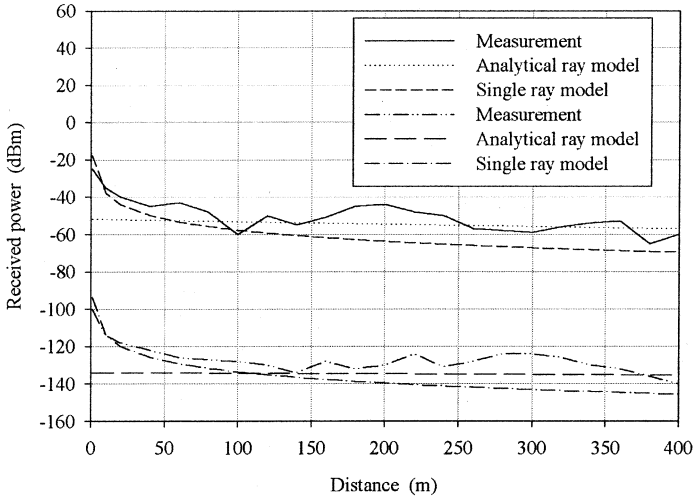

Fig. 5. Measured and predicted received power at 945 MHz and 1.853 GHz in a subway tunnel (-70 dBm offset added to the 1.853 GHz propagation).

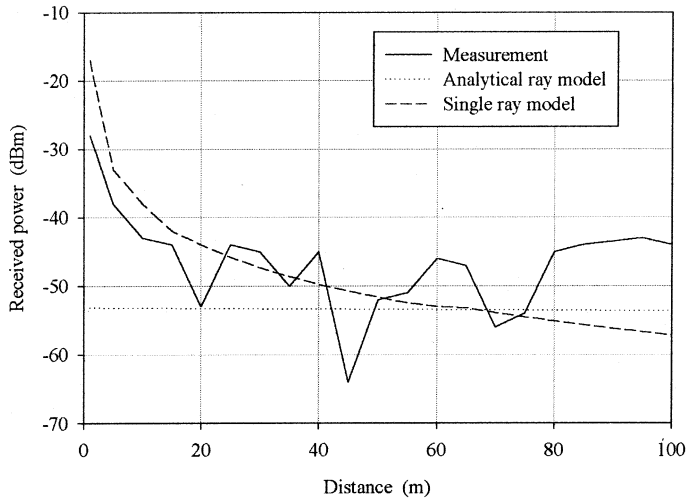

Fig. 6. Measured and predicted received power at 1.853 GHz in a subway tunnel.

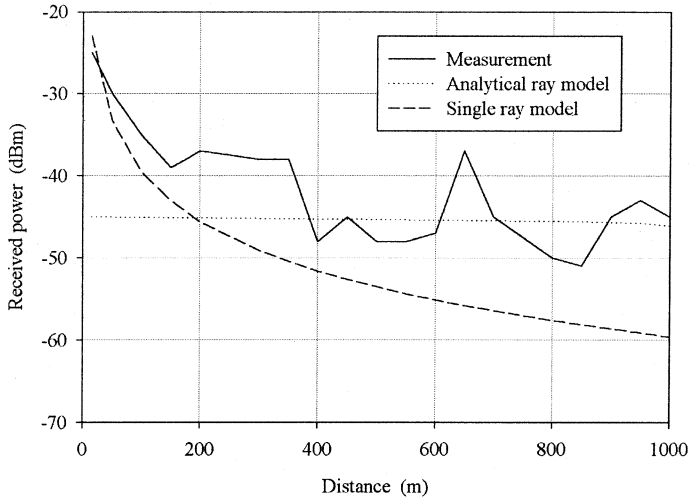

Fig. 7. Measured and predicted received power at 1.8 GHz in a road tunnel.

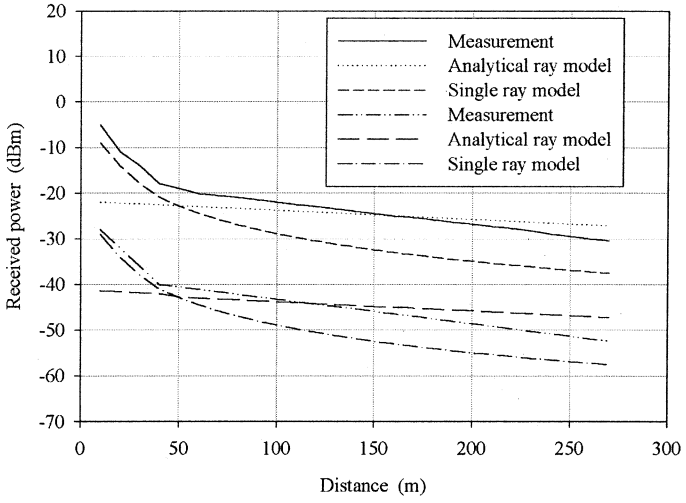

Fig. 8. Measured and predicted received power at 2.448 GHz in a coal mine tunnel.

calculated break points are at 60 m and 110 m, respectively. The predictions generally follow the measurements in both regions. Furthermore, the comparison of the propagation at 945 MHz and 1.853 GHz indicates that the location of the break point depends upon the frequency. Fig. 6 plots the prediction and the measurement for the propagation at 1.853 GHz in the rectangular subway tunnel with $w = 3.8$ m, $h = 4.3$ m, and $z = 110$ m. The calculated break point is at the distance of 75 m. The measurement was, thus, made largely in the near region; only the single ray optical model of our tunnel-propagation model is adequate for the prediction of the propagation.

A measurement at 1800 MHz in a tunnel of $w = 8.4$ m and $h = 7.2$ m is compared with the prediction in Fig. 7. For this measurement, the transmitting and receiving antennas were horizontally polarized and located at $(0, 0, z_o)$ and $(0.1w, 0, z)$, respectively. It is evident from the figure that the measured break point is at the distance of approximately 178 m and the calculated break point is at the distance of 193 m. In the prediction, the material parameters for this tunnel corresponded to concrete $\varepsilon_r = 5.5$ and $\sigma = 0.01$ S/m [4]. The prediction is within 6 dB of the measurement in the region before the break point and 8 dB in the region after the break point. Measurements at 2.448 GHz in a mine tunnel for two types of antennas were reported [16]. Fig. 8 illustrates the comparisons between the measurements and predictions. The errors between the predictions and the measurements are less than 5 dB. As expected, the received signal level for high-gain (12 dBi) directional antennas is much stronger than that of low-gain (2 dBi) omnidirectional ones. Note that for both cases the measured break points are at the distance of 45 m and the calculated break point at 50 m, which indicates that the location of the break point does not depend upon the antenna gain.

Table I lists the measured and calculated locations of the break points from Figs. 5 to 8. The locations of the break points estimated by the formula for urban microcells are also included for comparison [1]. It is interesting to note that our model yields more accurate locations of the break points for tunnel microcells. The formula for urban microcells is inapplicable for tunnel microcells.

Having validated the model, we can now use it to study the location of the break point in tunnel environments. Fig. 9 shows the

TABLE I
LOCATIONS OF THE BREAK POINTS

BP Locations / Tunnels	Measured Break Point (m)	Calculated Break Point (m)	Estimated Break Point (m)
Coal Mine Tunnel 900 MHz	40	40	29
Road Tunnel 900 MHz		150	31
Potash Mine Tunnel 915 MHz [14]	40	40	22
Arched Subway Tunnel			
945 MHz	68	60	46
1.853 GHz [15]	120	110	89
Rectangular Subway Tunnel 1.853 GHz [15]		75	80
Railroad Tunnel 1800 MHz	178	193	310
Coal Mine Tunnel 2.448 GHz [16]	45	50	59

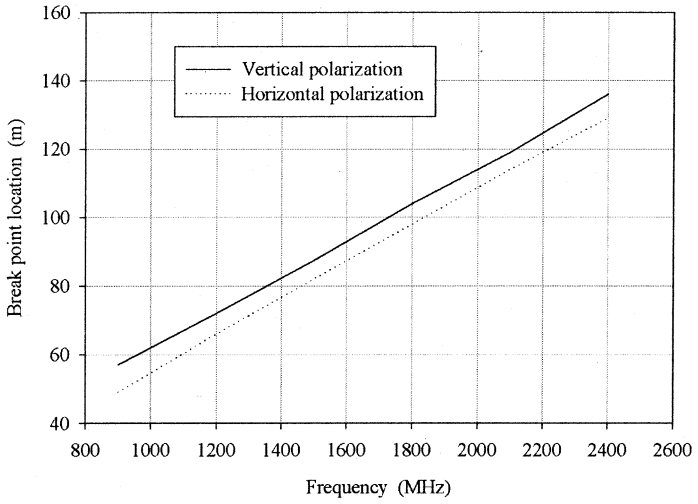

Fig. 9. Locations of the break point versus frequency with Tx antenna at $(0, 0, z_o)$ and Rx antenna at $(0, 0, z)$.

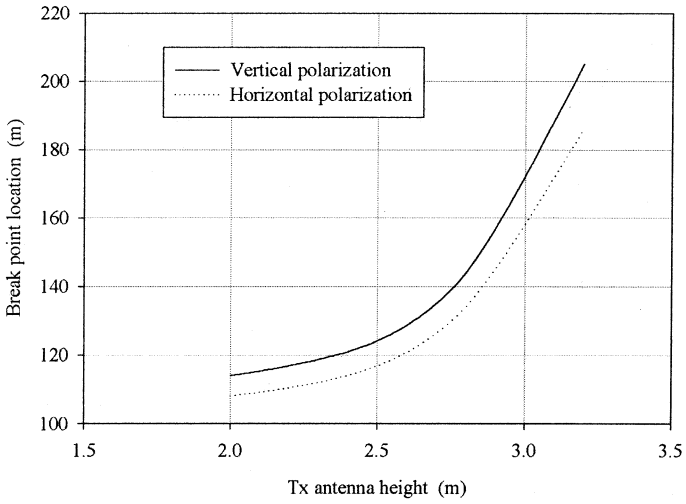

Fig. 10. Locations of the break point versus the antenna position with Tx antenna at $(0, y, z_o)$ and Rx antenna at $(0, 0, z)$.

locations of the break point as functions of frequency for vertical and horizontal polarization in the tunnel used in Fig. 1. The gain of the transmitting and receiving antennas is 2 dBi. As shown, the locations of the break point are correlated strongly with frequency; they move further away from the transmitting antenna as the frequency increases. This calculated frequency dependence is consistent with measurements shown in Fig. 5. Also, it is consistent with the Fresnel zone theory that states that the zone clearance is directly proportional to the frequency. Fig. 10 illustrates the dependence of the location of the break point on the antenna position in the tunnel. It is seen that the antenna position greatly affects the location of the break point. For instance, the location of the break point goes further as the transmitting antenna is closer to the tunnel ceiling. This is because the antenna closer to the ceiling causes a larger coupling loss to the dominant waveguide mode; as a result, it takes a longer distance for the dominant mode to become stronger. Fig. 11 displays the influence of the tunnel-transversal dimension on the location of the break point. Note that the location of the break point is highly related with the tunnel-transversal dimension. The larger the dimension is, the further the location of the break point is away from the transmitting antenna. This is the result of a larger cross-sectional tunnel being closer to a free space. In addition, it is found that the antenna gain has no effect on the location of the break point in the tunnel.

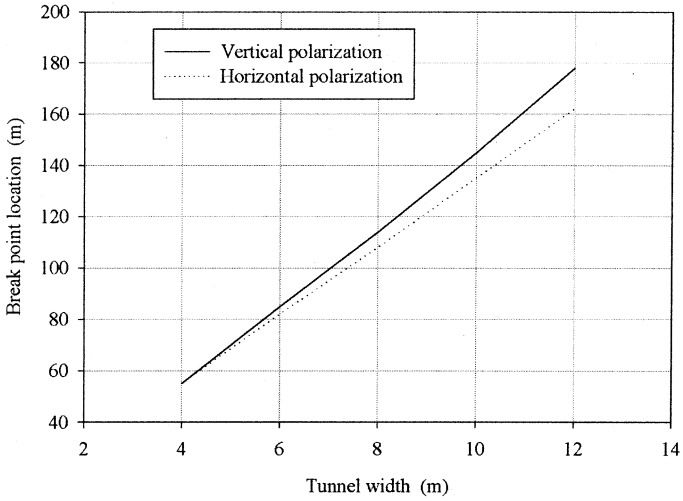

Fig. 11. Locations of the break point versus the tunnel transversal dimension with Tx antenna at $(0, 0, z_o)$ and Rx antenna at $(0, 0, z)$.

IV. Conclusion

Two propagation regions were observed for LOS topographies in tunnels. A novel model that can distinguish these propagation regions and predict their respective propagation losses was proposed. It was verified with measurements and then was used to study the effects of frequency, antenna parameters, and tunnel measures on the location of the break point. It was found for the first time that the location of the break point depends strongly upon frequency, antenna position, and tunnel-transversal dimensions. Higher frequencies, corner antenna positions, and larger tunnel-transversal dimension resulted in the location of the break point further away from the transmitting antenna. There was no effect of the antenna gain on the location of the break point.

Appendix
Derivation of the Coupling Loss of an Antenna in a Tunnel

Let us consider an antenna located at point (x, y) in a tunnel cross section. The power that the antenna receives or transmits is given by

$$P_r = A_e S(x, y) \tag{A1}$$

where A_e is the effective area of the antenna and $S(x, y)$ is Poynting's vector [4]. One can express A_e as

$$A_e = \frac{G\lambda^2}{4\pi} \tag{A2}$$

and $S(x, y)$ as

$$S(x, y) = \frac{1}{2}\eta_o \cos^2\left(\frac{\pi x}{w}\right)\cos^2\left(\frac{\pi y}{h}\right) \tag{A3}$$

where G is the antenna gain, λ is the wavelength, and η_o is the free space characteristic impedance. The power, calculated as the flux of this vector through the tunnel cross section, is given by

$$P = \frac{\eta_o wh}{4}. \tag{A4}$$

The coupling loss of the antenna is defined as

$$\begin{aligned}\text{CL (dB)} &= 10\log\left(\frac{P}{P_r}\right)\\ &= 10\log\left(\frac{2\pi wh}{\lambda^2 G}\cos^{-2}\left(\frac{\pi x}{w}\right)\cos^{-2}\left(\frac{\pi y}{h}\right)\right).\end{aligned} \tag{A5}$$

Taking an antenna of gain 2 dBi at 2 GHz in a tunnel of $w = 8$ m and $h = 5$ m as an example, we find that CL is 38, 41, and 44 dB for the antenna located at (0, 0), (0, 0.25 h), and (0.25 w, 0.25 h) in the tunnel cross section, respectively. Finally, it should be noted that (A5) does not remain accurate when the antenna is located close to the tunnel wall.

References

[1] H. H. Xia, H. L. Bertoni, L. R. Maciel, A. L. Stewart, and R. Rowe, "Radio propagation characteristics for line-of-sight microcellular and personal communications," *IEEE Trans. Antennas Propagat.*, vol. 41, pp. 1439–1447, Oct. 1993.

[2] M. J. Feuertein, K. L. Blackard, T. S. Rappaport, S. Y. Seidel, and H. H. Xia, "Path loss, delay spread, and outage models as functions of antenna height for microcellular system design," *IEEE Trans. Veh. Technol.*, vol. 43, pp. 487–497, Aug. 1994.

[3] Y. Deryck, "Natural propagation of electromagnetic waves in tunnels," *IEEE Trans. Veh. Technol.*, vol. 27, pp. 145–150, Aug. 1978.

[4] P. Delogne, *Leaky Feeders and Subsurface Radio Communications*. London, U.K.: Peter Peregrinus, 1982.

[5] T. Klemenschits and E. Bonek, "Radio coverage of road tunnels at 900 and 1800 MHz by discrete antennas," *Proc. 5th IEEE Int. Symp. Pers., Indoor, and Mobile Radio Commun.*, vol. 2, pp. 411–415, Sept. 18–22, 1994.

[6] M. Lienard and P. Degauque, "Propagation in wide tunnels at 2 GHz: A statistical analysis," *IEEE Trans. Veh. Technol.*, vol. 47, pp. 1322–1328, Nov. 1998.

[7] Y. Hwang, Y. P. Zhang, and R. G. Kouyoumjian, "Ray-optical prediction of radio wave propagation characteristics in tunnel environments, part one: Theory," *IEEE Trans. Antennas Propagat.*, vol. 46, pp. 1328–1336, Sept. 1998.

[8] Y. P. Zhang, Y. Hwang, and R. G. Kouyoumjian, "Ray-optical prediction of radio wave propagation characteristics in tunnel environments, Part two: Analysis and measurements," *IEEE Trans. Antennas Propagat.*, vol. 46, pp. 1337–1345, Sept. 1998.

[9] S. H. Chen and S. K. Jeng, "SBR image approach for radio wave propagation in tunnels with and without traffics," *IEEE Trans. Veh. Technol.*, vol. 45, pp. 570–578, Aug. 1996.

[10] S. F. Mahmoud and J. R. Wait, "Geometrical optical approach for electromagnetic wave propagation in rectangular mine tunnels," *Radio Science*, vol. 9, no. 12, pp. 1147–1158, 1974.

[11] Y. P. Zhang, "Characterization of Tunnel UHF Radio Propagation Channels for Microcellular and Personal Communications," Ph.D. Dissertation, Dept. Elect. Eng., Chinese University of Hong Kong, Hong Kong, China, 1995.

[12] A. G. Emslie, R. L. Lagace, and P. F. Strong, "Theory of the propagation of UHF radio waves in coal mine tunnels," *IEEE Trans. Antennas Propagat.*, vol. 23, pp. 192–205, Mar. 1975.

[13] Y. Yamaguchi, T. Abe, T. Sekiguchi, and J. Chiba, "Attenuation constants of UHF radio waves in arched tunnels," *IEEE Trans. Microwave Theory Tech.*, vol. 33, pp. 714–718, Aug. 1985.

[14] B. L. F. Daku, W. Hawkins, and A. F. Prugger, "Channel measurements in mine tunnels," *Proc. IEEE Veh. Technol. Conf. (VTC) '02*, pp. 380–383, 2002.

[15] D. Didascalou, J. Maurer, and W. Wiesbeck, "Subway tunnel guided electromagnetic wave propagation at mobile communications frequencies," *IEEE Trans. Antennas Propagat.*, vol. 49, pp. 1590–1596, Nov. 2001.

[16] H. Reuters, "Investigations on propagation of GHz radio waves in underground roadways," *Mining Technol.*, no. 10, pp. 447–451, 1982.

Y. P. Zhang received the B.E. degree from Taiyuan Polytechnic Institute, Shanxi, China, in 1982 and the M.E. degree from Shanxi Mining Institute, Taiyuan University of Technology, Shanxi, China, in 1987 and the Ph.D. degree from the Chinese University of Hong Kong, Hong Kong, in 1995, all in electronic engineering.

He was with Shanxi Electronic Industry Bureau (1982–1984), the University of Liverpool, Liverpool. U.K., (1990–1992), and the City University of Hong Kong (1996–1997). He taught at Shanxi Mining Institute (1987–1990) and the University of Hong Kong (1997–1998). He was a Full Professor at Taiyuan University of Technology from 1996 to 1998. He is now an Associate Professor of the School of Electrical and Electronic Engineering, Nanyang Technological University, Singapore. He has been involved in the areas of propagation of radio waves, characterization of radio channels, miniaturization of antennas, and implementation of wireless communications systems. He is currently working with his nine graduate students at the Integrated Systems Research Laboratory to develop circuits and components required to implement highly integrated wireless transceivers operating above 2 GHz using advanced packaging and silicon IC technologies.

Dr. Zhang received the Sino-British Technical Collaboration Award in 1990 for his contribution to the advancement of subsurface radio science and technology, an Overseas Research Students Award in 1992 from the Committee of Vice-Chancellors and Principals of the Universities of the United Kingdom, and an Excellent Graduate Award in 1995 from the Chinese University of Hong Kong. He also received the Best Paper Award from the Second International Symposium on Communication Systems, Networks and Digital Signal Processing, July 18–20, 2000, Bournemouth, U.K. He is listed in Marquis *Who's Who in Science and Engineering*.